Ceramics International 43 (2017) 11318–11323

Contents lists available at ScienceDirect

Ceramics International

journal homepage: www.elsevier.com/locate/ceramint

Optimization of colloidal nanosilica production from expanded perlite using Taguchi design of experiments

Zohreh Asadi, Reza Norouzbeigi*

School of Chemical, Petroleum and Gas Engineering, Iran University of Science and Technology, Narmak, Tehran, Iran

ARTICLE INFO

Keywords:
Colloidal nanosilica
Peptization
Perlite
Taguchi design

ABSTRACT

Colloidal nanosilica was prepared from perlite in two stages: production of wet gel and thermal peptization. The influence of acidic and alkaline solutions concentration, temperature and pH of the gel were investigated in wet gel production using Taguchi design of experiments. Effect of the temperature of the peptization process was studied by full factorial design. The purity of the obtained silica gel was analyzed using X-ray fluorescence (XRF) and the colloidal silica was characterized by dynamic laser scattering (DLS), field emission scanning electron microscope (FESEM) and N_2 sorption analyses. Results showed that pure colloidal nanosilica with purity of 99% was produced and the particle size of the product was in the range of 8 nm and 74 nm. Specific surface area of dried optimized mesoporous sample was 74.28 m^2/g.

1. Introduction

Colloidal silica has wide applications from binder in cement [1], coating in textiles [2], polishing of silicon wafer [3], catalyst precursor and support, paper fractionizing [4] to drug delivery systems in biotechnology [5]. Due to its divers and growing usages, various processes have been developed for production of colloidal silica, such as ion exchange [6], direct oxidation [7], peptization [8], dialysis, electro-dialysis and acid neutralization [9]. In this field, ion exchange is the most used process, but recycle of ion exchange resins are financially and environmentally a crucial problem. Furthermore, some residual Na might remain in product and it may reduce the purity and stability of colloid [9,10].

Peptization of wet silica gel in an alkaline solution is also a simple and practical method. There are two kinds of peptization processes: Thermal and ultrasonic-assisted. In ultrasonic-assisted method, releasing energy produced from collapsing of bubbles leads to peptization of gel, while in the thermal method heating results peptization [11,12]. Thermal peptization has been proposed by Thomas Graham [11] and Trail [13]. They investigated the effects of autoclave dimension and filled ratio. It was concluded that if there is no live steam, a tight 90% filled ratio is more suitable for peptization. White [14] concluded that suitable temperature and pressure for thermal peptization are 80–200 °C and 7–225 pound per square inch or higher, respectively. Ahlberg and Simpson [15] used two steps thermal peptization for the first time. However, some factors influencing two steps thermal peptization efficiency have been investigated by Rhee et al. [16]. They studied the effect of silica source concentration, pH of the gelling, the aging time and duration of the peptization. It has been found out that peptization efficiency could be promoted in 1 h aging time, 10% concentration of silica source, and pH of 10.5. Moreover, in first step of thermal peptization, after 10 h the efficiency was fixed. They also showed that acidic washing condition was more suitable for having pure products. On the other hand, one of the crucial factors affecting the final product cost is the raw material. Most of the current fabrication processes use almost expensive initial precursors. Fortunately, there are many low cost and available minerals which can be used as silica-containing resources. Reasonably, many researchers have been used low cost minerals such as olivine, vermiculite and chrysotile to produce nanosilica [17–20]. However, most of the mineral based synthetized nanosilicas reported till now, are powdered and as we know, there many few reports on colloidal nanosilica from a mineral source. In this study, perlite has been selected as a low cost silica-containing mineral for the first time. It's a glassy volcanic rock which expands 10–20 times at temperature in range of 760–1100 °C and contains about 70% silica [21]. Major producers of perlite are Greece, Turkey and United States. Perlite is also abundantly available in Iran so it is a reasonable and low cost Si source as a precursor [22]. This study is devoted to use perlite as inexpensive raw material and optimization of the effects of some important parameters affecting the final colloidal nanosilica product via Taguchi method and full factorial design of experiment. The fabrication process has two parts: purification and thermal peptization. Influential factors are acid solution concentration, alkaline solution concentration and temperature, pH of gel and

* Corresponding author.
E-mail address: norouzbeigi@iust.ac.ir (R. Norouzbeigi).

http://dx.doi.org/10.1016/j.ceramint.2017.05.332
Received 8 April 2017; Received in revised form 24 May 2017; Accepted 27 May 2017
Available online 29 May 2017

temperatures of the peptization steps. As the particle size of the prepared nano silica has a great impact on the stability of the colloids, fabrication of pure colloidal nano-silica with smaller particle size was target of the research.

2. Material and methods

2.1. Material

Expanded perlite was purchased from a local company (Zamin Kav Co., west Azerbaijan province, Iran) with composition given in Table 1. Perlite grains were passed through #100-U.S. mesh size so the initial particle size was less than 150 μm. Other materials including sodium hydroxide pellets (97%), sulfuric acid (Analytical grade, 95–97%), hydrochloric acid (Analytical grade, 37%) were provided from Merck Company and were used without any purification.

2.2. Preparation of colloidal nanosilica

2.2.1. Wet gel production

The experiments were designed by 3-level L_9 Taguchi orthogonal array, which helps in reducing the number of experiments. In the Taguchi statistical design, the introduced orthogonal arrays can supply efficient and suitable possibility to perform the practical tests with the minimum number of examinations. The wet gel production influential factors were hydrochloric acid concentration, alkaline reaction temperature, sodium hydroxide concentration, and pH of the gel production. The controlling parameters and their levels are introduced in Table 2.

For production of wet gel, 5 g of washed and calcined perlite (800 °C for 3 h) had been reacted with 100 ml hydrochloric acid at 80 °C for five hours. Eq. (1) shows the related reaction. Where M can be Al, Mg, Ca, Na, and Fe and n is the valence of the elements. Then, settled materials were separated and washed from soluble impurities by filtering over a Buchner funnel, using Whatman No. 41 filter papers. Subsequently, the residual was dried for 12 h at 110 °C, and then reacted with 100 ml sodium hydroxide aqueous solution for 90 min. Sodium silicate solution and hydroxides of the impurities were products of this alkaline step. It is shown in Eq. (2). The separation operation done in the alkaline step was in the same way of acidic one. Both of acidic and alkaline processes were carried out in a reflux system. Consequently, 2.5 M sulfuric acid aqueous solution was added to the sodium silicate solution under continuous and constant rate of stirring to reach desired pH of wet silica gel. As expressed in Eq. (3) sodium sulfate is the byproduct of the reaction. For elimination of the byproduct, the wet gel was first washed by 150 ml of sulfuric acid aqueous solution (0.1 M) and then washed by distilled water until the gel pH reached about 7. Finally, Wet gel was dried for characterization.

$$\text{Perlite} + HCl \rightarrow M(Cl)_n + SiO_2\downarrow \quad (1)$$

$$SiO_2 + 2NaOH \rightarrow Na_2SiO_3 + H_2O \quad (2)$$

$$Na_2SiO_3 + H_2SO_4 \rightarrow SiO_2 + Na_2SO_4 + H_2O \quad (3)$$

Nine experiments were carried out according to the rows of the experimental design (Table 3). After statistical analysis and specifying optimized combination of factors and levels of wet silica gel production, the experiments were continued with thermal peptization of the obtained gel.

2.2.2. Peptization of wet gel

Initially, the wet gel was aged 1 h. Then 100 ml of sodium hydroxide solution (0.1 M) was added to the gel, under vigorous stirring for 1 h. To result more stable products, a two-steps thermal peptization process was used. A tight Teflon tube used as a reactor and it was put in a furnace with specific thermal program. The durations of the first and second steps were one and 10 h respectively. The effect of temperatures of the first and the second steps were investigated using a two-parameter full factorial design. The effective parameters and their levels are introduced in Table 4. Table 5 shows combination of the factors and levels. Accordingly four experimental runs were done. Process of colloidal nanosilica production, is schematically shown in Fig. 1.

2.3. Characterizations

To determine the chemical composition of the raw perlite and dried resulted silica gels, X-ray fluorescence (XRF) were applied using a Philips, PW 1800 device. Particle size distribution and zeta potential are two crucial features of the products. Average particle size and the poly disparity index (PDI) represent the quality of the product. The lower PDI shows narrower particle size distribution. The aim of the optimization was to achieve smaller particle sizes. Furthermore, stability of the colloid is a substantial property for practical production

Table 1
Chemical composition of the raw expanded perlite.

Component	wt%
SiO_2	74.9
Al_2O_3	14.2
Na_2O	4.1
K_2O	3.4
MgO	1.5
CaO	1.2
Fe_2O_3	0.7

Table 2
Wet gel production parameters and their levels.

Symbol	Wet gel production parameter	Unit	Level 1	Level 2	Level 3
A	Hydrochloric acid concentration	M	3	4	5
B	Alkaline step temperature	°C	70	80	90
C	Sodium hydroxide concentration	M	4.5	3.5	2.5
D	pH of Gel	–	7	8	9

Table 3
Taguchi experimental design (factors-levels combination).

Run	Factors				Response	
	A	B	C	D	Y_i	Silica purity (%)
1	1	1	1	1	Y_1	92.86
2	1	2	2	2	Y_2	96.48
3	1	3	3	3	Y_3	97.80
4	2	1	2	3	Y_4	98.50
5	2	2	3	1	Y_5	97.83
6	2	3	1	2	Y_6	98.00
7	3	1	3	2	Y_7	95.55
8	3	2	1	3	Y_8	96.20
9	3	3	2	1	Y_9	93.50

Table 4
Peptization step parameters and their levels.

Symbol	Peptization parameter	Level −1	Level +1
F	First step temperature (°C)	100	120
G	Second step temperature (°C)	160	180

Table 5
Full factorial experiment design (the thermal peptization step).

Run	Factors			Response	
	F	G	F × G	Y_i	Average particle size (nm)
1	−1	1	−1	Y_1	61.2
2	1	−1	−1	Y_2	113
3	−1	−1	1	Y_3	40.6
4	1	1	1	Y_4	65.0

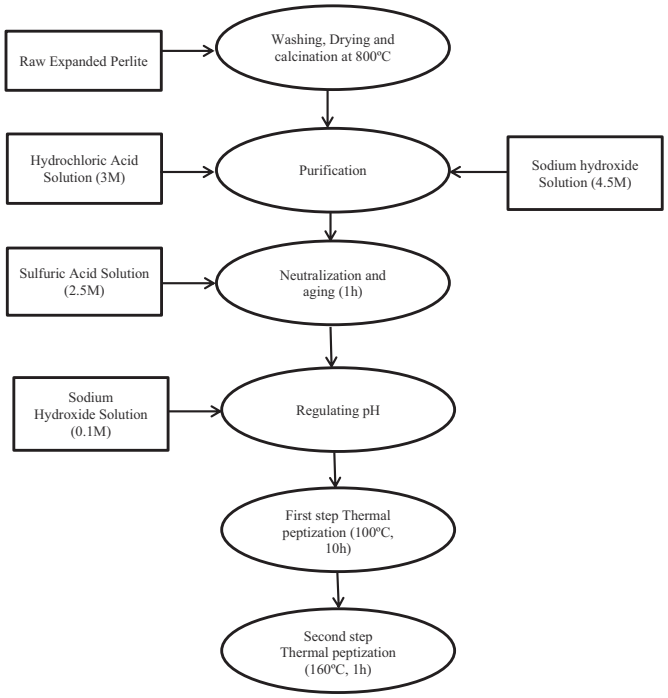

Fig. 1. Schematic process flow diagram of colloidal nanosilica production.

and application of the colloidal nanosilica. Zeta potentials more than +30 mV or less than −30 mV indicate stable colloids [23]. Both dynamic light scattering (DLS) analysis and zeta potential measurements were performed using a Malvern light scattering unit, zetasizer Nano ZS (red badge) ZEN 3600 with a 633 nm He–Ne laser.

Obtained colloidal nanosilica samples were dried at 80 °C for 10 h, for the other characterization such as field emission scanning electron microscopy (FESEM) and gas physisorption. FESEM (Zeiss, sigma) studies were operated at 30 kV for morphological analysis. Besides, the specific surface area of the best sample was measured by a NOVA® Station B Surface Area Analyzer using N_2 sorption method and the Brunauer–Emmett–Teller (BET) isotherm model.

3. Results and discussion

3.1. Wet gel production

The weight percentage of silica was considered as response of Taguchi experimental design. Results are given in Table 3. The XRF results are presented in Table 6. In Taguchi design, effect of the factors, parameters ranking and optimal conditions can be evaluated and introduced by so called standard (the main effect of means, E_f) method and analysis of variance (ANOVA) [23].

For calculation of E_f, the mean value of responses should be determined for every level of the factor. Finally, the factor effect can be obtained by subtracting the lowest computed mean value from the highest one [24]. For instance the effect of factor A was calculated according to Eq. (4).

$$\begin{aligned} \overline{A_1} &= \frac{Y_1+Y_2+Y_3}{3} = \frac{92.86+96.48+97.80}{3} = 95.69\% \\ \overline{A_2} &= \frac{Y_4+Y_5+Y_6}{3} = \frac{98.50+97.83+98.00}{3} = 98.11\% \\ \overline{A_3} &= \frac{Y_7+Y_8+Y_9}{3} = \frac{95.55+96.20+93.53}{3} = 95.08\% \\ E_{fA} &= \overline{A_2}-\overline{A_3} = 98.11-95.08 = 3.03\% \end{aligned} \quad (4)$$

The effect of parameters B, C and D are 1.20%, 1.37% and 2.77% respectively. A parameter with higher E_f has more influence on the response changes [25]. Computed factor effects and factor ranking are presented in Table 7. According to Table 7, Factor A (HCl solution concentration) can be considered as the most influential parameter as ranked 1. Consequently, pH of gel, temperature of alkaline reaction step and concentration of the sodium hydroxide solution can be ranked respectively. Fig. 2 shows factors main effect plot. Hence, higher purity of silica is desired the highest mean value of a level, shows the best studied condition. According to Fig. 2, the optimum sample will be achieved by combination of A2, B2, C3 and D3.

Analysis of variance reveals contribution of each factor (Table 8). It shows that acidic solution concentration and pH are the most important factors, because the contribution percentages of these two factors are significantly higher than others. This result confirms the previous standard factor effect output given in Table 7. As it is shown in Table 3 the most purified sample was produced in the fourth experimental run (98.5%). In this experiment in which the concentrations of acid and gelation pH values (most effective factors) were fixed at the optimum levels (2 and 4 correspondingly), the purity of the resulted product was maximum.

Finally, the response of the run carried out under optimized conditions can be predicted in Taguchi design [25]. The predicted silica weight percent can be calculated by Eqs. (5) and (6).

$$Y_{opt} = \overline{Y} + (\overline{A_2}-\overline{Y}) + (\overline{B_2}-\overline{Y}) + (\overline{C_3}-\overline{Y}) + (\overline{D_3}-\overline{Y}) = 100.197\% \quad (5)$$

whereas:

$$\overline{Y} = \sum_1^9 Y_i/9 \quad (6)$$

In these equations $\overline{Y}$ is the grand average of responses and Y_{opt} is the estimated response value of the optimized sample. For evaluation of the estimation error a confirmation test should be conducted under the optimal conditions. The XRF result of the confirmation experiment is given in Table 9. As the purity of the optimum sample was 99.01%, so the absolute error of the prediction was about 1.18%. Statistically, this low error value proves the accuracy and reproducibility of the results well. According to statistical assessments, optimum acid solution concentration is 4 M. By increasing acid concentration from 4 M to 5 M, the purity decreased. Diffusion of H^+ to solid phase is necessary for solution of impurities, so it seems that after the optimum acid concentration value, released cations repel H^+. Similar trend has been reported in extraction of alumina from clays [26].

Reaction temperature of 90 °C and solution concentration of 2.5 M can be considered as the optimized conditions for the alkaline step. In alkaline conditions alumina and silica have tendency of forming polysialate or aluminosilicate oxides [27]. Antonnucci [28] and Krol [29] showed that zeolite (aluminosilicate oxides) can be produced from perlite in the alkaline solutions. These studies indicate that at temperatures near to 90 °C and high alkaline concentrations (for instance solid/liquid ratio of 1:4) more zeolite is produced. The proposed levels are in compliance with other results. The fact can be described sedimentation of silica based on the higher reaction temperature and sodium hydroxide concentration which leads to reduction of the produced silica gel purity. The pH value should be set at the optimized amount of 11 for the gel production. Decreasing of pH in neutralization step leads to more siloxane bonds formation. It causes a

Table 6
XRF elemental analysis.

Experiment No.	Al_2O_3 (%)	CaO (%)	SO_3 (%)	MgO (%)	Fe_2O_3 (%)	Na_2O (%)
1	5.56	0.55	0.7	0.27	0.06	0
2	2.83	0.2	0.27	0.12	0.08	0.02
3	1.43	0.23	0.24	0.21	0.06	0.03
4	0.47	0.21	0.22	0.41	0.16	0.03
5	1.46	0	0.25	0.41	0.02	0.03
6	1.26	0	0.25	0.44	0.02	0.03
7	3	0.35	0.27	0.76	0.03	0.04
8	2.46	0.24	0.24	0.77	0.04	0.05
9	5.13	0.34	0.25	0.67	0.06	0.05

Table 7
Ef and factors ranking (Taguchi L9 design).

Level	Factor			
	A	B	C	D
1	95.71	95.64	95.69	94.73
2	98.11	96.84	96.16	96.68
3	95.08	96.43	97.06	97.50
E_f	3.03	1.2	1.37	2.77
Rank	1	4	3	2

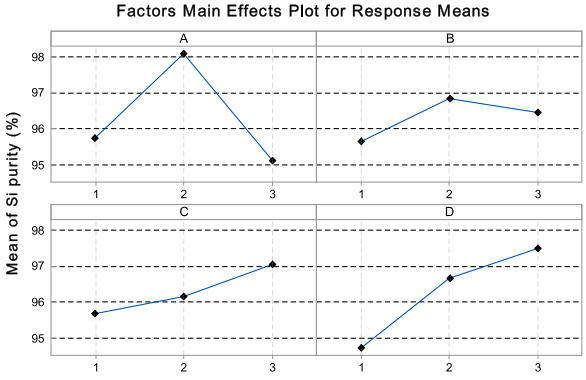

Fig. 2. Wet gel production factors main effect plot.

Table 8
ANOVA table for Taguchi L_9 designed experiments.

Source of variance	Sum of squares	DOF	Mean square	Contribution (%)
A	15.3016	2	7.6508	46.94
B	2.2374	2	1.11868	6.86
C	2.9201	2	1.4600	8.96
D	12.1403	2	6.0701	37.24
Error	0.0000	–	–	–
Total	32.5994	8	–	–

Table 9
XRF results for the optimized sample (confirmation test).

Component	SiO_2	Al_2O_3	MgO
Weight percent (%)	99.01	0.90	0.09

condensed gel structure and hence the trapped ions can't be removed from the gel in the washing step [16]. Rhee and coworkers [16] showed that the optimized pH value for silica gel peptization is 10.

Process yield of silica purification for each experiment have been calculated by Eq. (7).

$$PY_i(\%) = m_{SiO_2,i}/m_{SiO_2,0} \quad (7)$$

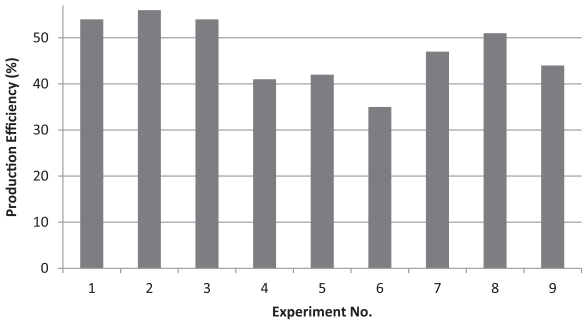

Fig. 3. Wet gel production yield.

Where, PY_i and m_i are process yield of the ith experiment and Si mass value, respectively. Index i represents the experimental run number according to Table 3. Index 0 relates to the initial raw expanded perlite. The process yield is defined by division of dried silica gel mass and raw expanded perlite mass (5 g).

According to Fig. 3, the efficiency is more than 50% in first three experiments, and then it reduces about 10% in next three experiments. Finally, the efficiency increases slightly in last three experiments. Acid solution concentration is the major variable. It is determined by statistical analysis that acid concentration is the most effective factor and the amount of its optimum level is 4 M. This value was set for runs 4, 5 and 6. So it can be concluded that the next alkaline step began with a relatively more pure initial material in the mentioned runs. It implies that more silica is exposed to the sedimentation process in the experiments 4, 5 and 6. Reasonably the process yield would be decreased in such experimental runs.

3.2. Thermal peptization

The average particle size of the obtained colloidal nanosilica samples were selected as the response of the experiments (Table 5). Similar to the previous calculations, the effect of each parameter was calculated according to Eqs. (8)–(10) [23].

$$E_{fF} = Y_{F^+} - Y_{F^-} \quad (8)$$

$$E_{fG} = Y_{G^+} - Y_{G^-} \quad (9)$$

$$E_{fF\times G} = Y_{FG^+} - Y_{FG^-} \quad (10)$$

The calculated effects of factors F, G and interaction of them (F×G) are presented in Table 10. The resulted data show, the interaction of the first and the second step temperatures are significant, and the temperature of the first thermal peptization step is the most effective parameter.

Table 11 shows analysis of variance of the peptization parameters. ANOVA results confirm results of the main factor effect evaluation given in Table 10. The calculated mean square of the first step temperature is higher than others and as it was mentioned this factor can be considered as the most important controlling parameter [24]. As

Table 10
Ef and factors ranking (Full Factorial Design).

Level	Factor		
	F	G	F × G
+1	89	63.1	52.8
−1	50.9	76.8	87.1
E_f	38.1	−13.7	−34.3
Rank	1	3	2

Table 11
ANOVA results for full factorial design of experiments.

Source of variance	Sum of square	DOF	Mean square
F	1451.6	1	1451.6
G	187.7	1	187.7
FG	1176.5	1	1176.5
Error	0.0	0	–
Total	28.15.8	3	–

it has been reported, the temperature of the first step has the crucial role on the particle preparation and the second step temperature affects mainly the product stabilization [16].

For analysis of the average particle size and particle size distribution DLS analysis was carried out. Results are shown in Fig. 4. The smallest resulted average particle size was occurred in the experiment 3. The highest one was obtained in experiment 2. This fact shows that lower temperature difference between two steps leads to a lower average particle size and visa verse. It can be seen from Fig. 4 that the experiments 1 and 4 of Table 5, which have been done under the similar temperature differences, resulted almost similar average particle sizes and particle size distributions.

Polydispersity index (PDI) is a statistical parameter which is between 0 and 1. Lower PDI value indicates that the particle size distribution of the solids in the colloid medium is suitably narrow and it can be considered as an accepted colloid stability assessment criterion [12]. Fig. 5 displays PDI values of the achieved colloids. Considering experiments 3 and 4, it can be concluded that higher temperature differences between two peptization steps can lead to higher PDI values. Higher temperatures of the silica sols in alkaline regions promote the coarsening (Ostwald ripening) of the silica particles. Accordingly, smaller particles will sediment on the larger particles to make lager agglomerates [30]. In fact, lower differences between two stages temperatures lead to less sedimentation, particle size growth and instability of the nano-colloids.

Figs. 6 and 7 show FESEM micrographs of perlite and dried colloidal silica prepared in experiment 3. According to the figures, perlite has a layered structure and the final product has spherical

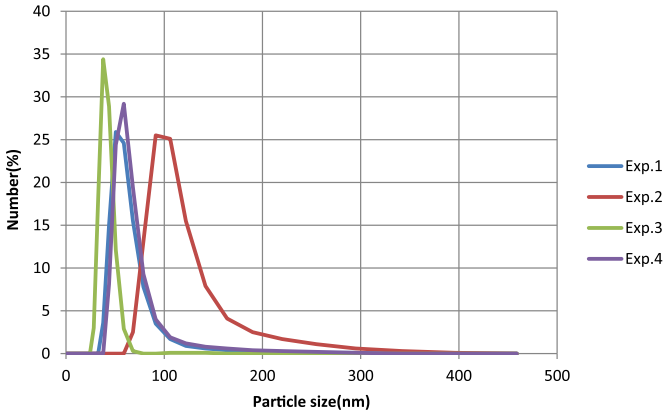

Fig. 4. Particle size distribution of colloidal silica samples in term of number.

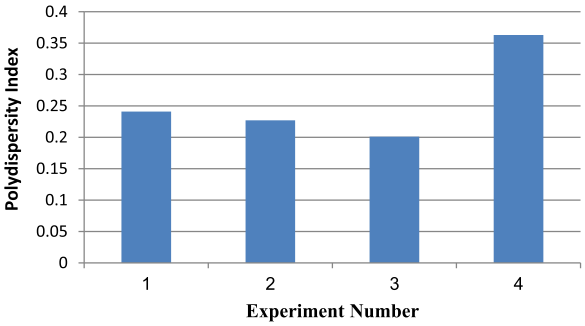

Fig. 5. Polydispersity index of colloidal samples.

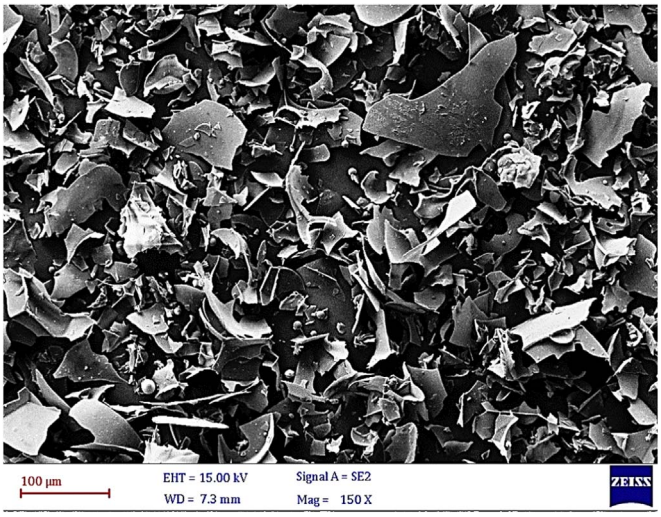

Fig. 6. FESEM of raw expanded perlite particles at 150× magnification.

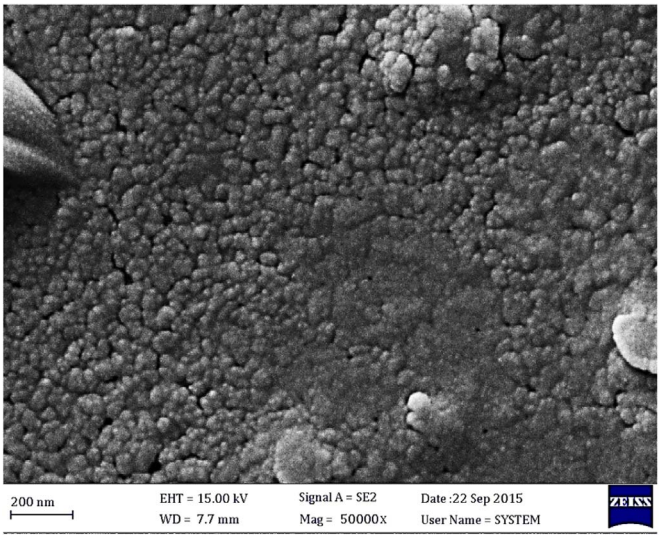

Fig. 7. FESEM micrograph of dried colloidal nanosilica at 80 °C from sample 3 at 50× magnification.

morphology. There are some aggregates including nano clusters. It can be related to the drying process which may promote the particle agglomeration. The result of N_2 sorption isotherm is shown in Fig. 8. This graph exhibited an isotherm of type IV with almost a hysteresis of H1. The isotherm curve indicates that dried colloidal silica can be considered mesoporous and the H1 loop may be related to the narrow distribution of fine particles and some agglomerates [30]. FESEM micrograph also confirms the presence of the aggregated clusters resulted from nitrogen adsorption and desorption analysis. The specific

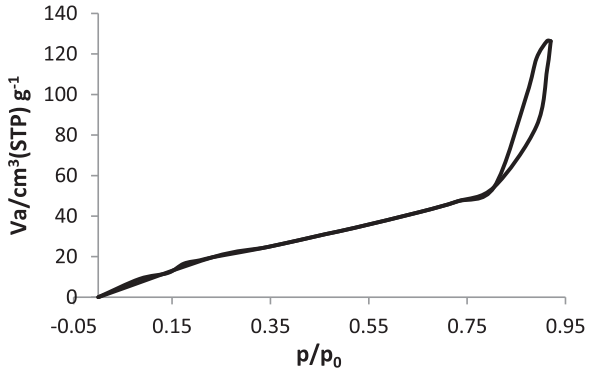

Fig. 8. N_2 adsorption-desorption isotherm for dried colloidal nanosilica of sample 3 at 80 °C.

surface area and mean pore diameter of sample 3 (the optimum sample) calculated from the BET and BJH models were 74.28 m^2/g and 2.27 nm, respectively. Similar N_2 sorption isotherm curves have been reported for nano-silica derived from other mineral sources [17,31]. Zeta potential of a colloid can determine the stability of colloid dispersion as another accepted key indicator [32]. The amount of the obtained colloidal nanosilica zeta potential resulted from the experiment 3 was −37.2 mv. A colloid having measured zeta potential greater than +30 mv or less than −30 mv has a suitable stability.

4. Conclusion

Pure colloidal nanosilica was produced from expanded perlite successfully. The optimized conditions for production of wet silica gel based on the parameters such as acid concentration, alkaline concentration, alkaline temperature and pH of gel production were 4 M, 2.5 M, 80 °C and 10, respectively. The optimized silica gel sample had about 99% purity. Optimized temperatures of thermal peptization steps were 120 °C and 160 °C. It was concluded that lower temperature differences lead to lower average particle sizes. Statistical analysis shows that acid solution concentration and temperature of the first step are the most effective factors. The resulted nano SiO_2 particle size was in the range of 8 and 74 nm. Process yield percentage obtained under optimized conditions was about 46%.

References

[1] J. Björnström, A. Martinelli, A. Matic, L. Börjesson, I. Panas, Accelerating effects of colloidal nano-silica for beneficial calcium-silicate-hydrate formation in cement, Chem. Phys. Lett. 392 (2004) 242–248.
[2] B. Mahltig, H. Böttcher, Modified silica sol coatings for water-repellent textiles, J. Sol.-Gel Sci. Technol. 27 (2003) 43–52.
[3] V.E. Gaishun, O.I. Tulenkova, I.M. Melnichenko, S.A. Baryshnin, Y.A. Potapenok, A.P. Xlebokazov, W. Stręk, Preparation and properties of colloidal nanosize silica dioxide for polishing of monocrystalline silicon wafers, Mater. Sci. 20 (2002) 19–22.
[4] H.E. Bergna, W.O. Roberts, Colloidal Silica: Fundamentals and Applications, Surfactant Science Series 131, CRC Press, New York, 2005.
[5] H.A.A. Wab, K.A. Razak, N.D. Zakaria, Properties of amorphous silica nanoparticles colloid drug delivery system synthesized using the micelle formation method, J. Nanopart. Res. 16 (2014) 22–56.
[6] M.S. Tsai, The study of formation colloidal silica via sodium silicate, Mater. Sci. Eng. 106 (2004) 52–55.
[7] W.K. Na, H.M. Lim, S.H. Huh, S.E. Park, Y.S. Lee, S.H. Lee, Effect of the average particle size and the surface oxidation layer of silicon on the colloidal silica particle through direct oxidation, Mater. Sci. Eng. *B* 163 (2009) 82–87.
[8] C.C. Legal, US Pat.2572578, 1955.
[9] M.J. Comstock, The Colloid Chemistry of Silica, Maple press, Washington, 1994.
[10] H.M. Lim, J. Lee, J.H. Jeong, S.G. Oh, S.H. Lee, Comparative study of various preparation methods of colloidal silica, Engineering 2 (2010) 998–1005.
[11] R.K. Iler, The Chemistry of Silica: Solubility, Polymerization, Colloid and Surface Properties, and Biochemistry, John Wiley & Sons Inc, New York, 1979.
[12] V. Jafari, A. Allahverdi, M. Vafaei, Ultrasound-assisted synthesis of colloidal nanosilica from silica fume: effect of sonication time on the properties of product, Adv. Powder Technol. 25 (2014) 1571–1577.
[13] H.S. Trail, US Pat.2572578, 1948.
[14] J.F. White, US Pat.2375738, 1945.
[15] J.E. Ahlberg, E.A. Simpson, US Pat.2900348, 1959.
[16] Y. Lee, Preparation of colloidal silica using peptization method, Colloids Surf. 173 (2000) 109–116.
[17] A. Lazaro, H.J.H. Brouwers, G. Quercia, J.W. Geus, The properties of amorphous nano-silica synthesized by the dissolution of olivine, Chem. Eng. J. 211–212 (2012) 112–121.
[18] M. Zhao, Z. Tang, P. Liu, Removal of methylene blue from aqueous solution with silica nano-sheets derived from vermiculite, J. Hazard. Mater. 158 (2008) 43–51.
[19] K. Liu, Q. Feng, Y. Yang, G. Zhang, L. Ou, Y. Lu, Preparation and characterization of amorphous silica nanowires from natural chrysotile, J. Non Cryst. Solids 353 (2007) 1534–1539.
[20] L. Wang, A. Lu, C. Wang, X. Zheng, D. Zhao, R. Liu, Nano-fibriform production of silica from natural chrysotile, J. Colloid Interface Sci. 295 (2006) 436–439.
[21] N. Tekin, Surface Properties of Poly (Vinylimidazole) -Adsorbed Expanded Perlite, 93, 2006, pp. 125–133.
[22] U.S. Geological Survey Mineral Commodity Summaries 2014, U.S. Geological Survey, 2014.
[23] D.C. Montgomery, Design and Analysis of Experiment, 5th ed., John Wily and sons, 2004.
[24] R.K. Roy, Design of Experiments Using the Taguchi Approach: 16 Steps to Product and Process Improvement, John Wiley & Sons Inc, New York, 2001.
[25] R. Norouzbeigi, M. Edrissi, Modification and optimization of nano-crystalline Al_2O 3 combustion synthesis using Taguchi L 16 array, Mater. Res. Bull. 46 (2011) 1615–1624.
[26] S. Arabia, Extraction of Alumina from Local Clays by Hydrochloric Acid Process, 20, 2009, pp. 29–41.
[27] F. Pacheco Torgal, J. Castro-Gomes, S. Jalali, Alkali-activated binders: a review, Constr. Build. Mater. 22 (2008) 1305–1314.
[28] P.L. Antonnucci, M.L. Crisafulli, N. Giordano, N. Burriesci, Zeolitization of perlite, Mater. Let. 3 (1985) 302–307.
[29] M. Król, W. Mozgawa, J. Morawska, W. Pichór, Spectroscopic investigation of hydrothermally synthesized zeolites from expanded perlite, Microporous Mesoporous Mater. 196 (2014) 216–222.
[30] A. Lazaro, M.C. van de Griend, H.J.H. Brouwers, J.W. Geus, The influence of process conditions and Ostwald ripening on the specific surface area of olivine nano-silica, Microporous Mesoporous Mater. 181 (2013) 254–261.
[31] P. Lu, Y. Lo Hsieh, Highly pure amorphous silica nano-disks from rice straw, Powder Technol. 225 (2012) 149–155.
[32] J. Jiang, G. Oberdorster, P. Biswas, Characterization of size, surface charge, and agglomeration state of nanoparticle dispersions for toxicological studies, J. Nanopart. (2009) 77–89.